

Alteration of Brain Type N-Glycans in Neurological Mutant Mouse Brain

Shin-ichi Nakakita^{1,2}, Shunji Natsuka¹, Jun Okamoto¹, Kazuhiro Ikenaka³ and Sumihiro Hase^{1,*}

¹Department of Chemistry, Graduate School of Science, Osaka University, Toyonaka, Osaka 560-0043; ²Department of Functional Glycomics, Life Science Research Center, Kagawa University, 1750-1 Ikenobe, Miki-cho, Kita-gun, Kagawa 761-0793; and ³Division of Neurobiology and Bioinformatics, National Institute for Physiological Sciences, Okazaki National Research Institutes, Okazaki, Aichi 444-0867

Received April 21, 2005; accepted June 3, 2005

We have previously detected two brain-specific and development-dependent N-glycans [H. Shimizu, K. Ochiai, K. Ikenaka, K. Mikoshiba, and S. Hase (1993) *J. Biochem.* 114, 334–338]. In the present study we attempted to analyze specific N-glycans detected in neurological mutant mice. N-glycans in cerebrum and cerebellum obtained from 3-week-old neurological mutant mice (*jimpy*, *staggerer*, and *shiverer*) were compared with those obtained from normal mice. N-glycans liberated from the cerebrum and cerebellum by hydrazinolysis-N-acetylation were pyridylaminated, and pyridylamino derivatives of N-glycans thus obtained were separated into neutral and five acidic fractions by anion exchange chromatography. PA-N-glycans in each fraction were compared with those obtained from normal mice by reversed-phase HPLC, and the following results were obtained. The ratio of the two brain-type N-glycans, Man α 1-3(GlcNAc β 1-2Man α 1-6)(GlcNAc β 1-4)Man β 1-4GlcNAc β 1-4(Fuca1-6)GlcNAc (BA-1) to GlcNAc β Man α 1-3(GlcNAc β 1-2Man α 1-6)(GlcNAc β 1-4)Man β 1-4GlcNAc β 1-4(Fuca1-6)GlcNAc (BA-2), was higher in *staggerer* mice than other mutant mice and normal mice. Sia-Gal-BA-2, triantennary N-glycans, and bisected biantennary N-glycans were found in the cerebellum of *shiverer* and *staggerer* mice but not in normal or *jimpy* mice. High-mannose type N-glycans were not altered in mutant mice brains. The amounts of disialylbiantennary N-glycans and disialylfucosylbiantennary N-glycans were lower in *jimpy* mouse cerebellum than in normal mouse cerebellum, but were higher in *shiverer* mouse. Some alterations of N-glycans specific to mutations were successfully identified, suggesting that expression of component(s) of the N-glycan biosynthetic pathway was specifically affected in neurological mutations.

Key words: central nervous system, mutant mice, N-glycan, pyridylation.

Abbreviations: ER, endoplasmic reticulum; Fuc, L-fucose; Gal, D-galactose; GlcNAc, N-acetyl-D-glucosamine; NCAM, neural cell adhesion molecule; Man, D-mannose; M_n, Man_nGlcNAc₂-PA; PA-, pyridylamino; Sia, N-acetylneuraminic acid. For abbreviations of N-glycans, see Fig. 3.

Neurological mutations affect processes associated with neural development and subsequently manifest as aberrant behavior. The study of neurological mutant mice provides new insights into both specific murine disease processes and mechanisms involved in the normal development of the mammalian central nervous system (1–4). For example, the cerebellum of *staggerer*, *shiverer*, *jimpy* mutant mice is dramatically affected and greatly reduced in size due to reduced numbers of various cell types. The most notable problem associated with the *staggerer* mutation is that purkinje cells fail to develop their mature dendritic trees (5). The *shiverer* mutation is associated with defects in the myelin of the central nervous system (6). The *jimpy* mutation is associated with death of oligodendrocyte cells and defective myelin in the central nervous system (7). We previously reported two N-glycans, Man α 1-3(GlcNAc β 1-2Man α 1-6)(GlcNAc β 1-

4)Man β 1-4GlcNAc β 1-4(Fuca1-6)GlcNAc (BA-1) to GlcNAc β Man α 1-3(GlcNAc β 1-2Man α 1-6)(GlcNAc β 1-4)Man β 1-4GlcNAc β 1-4(Fuca1-6)GlcNAc (BA-2), which are specifically expressed in mouse brain in a development-dependent manner (8, 9). They are expressed in large amounts and account for 5–7% of the total N-glycans in this tissue (8). BA-2 was subsequently found to be one of the major components in human β -trace protein and asialotransferrin from cerebrospinal fluid (10, 11). The presence of brain-specific N-glycans is due to the specificity of a β 1-4galactosyltransferase expressed in adult mouse brain (12). To investigate the functions of these N-glycans and to find other N-glycans specific to these mutations, we analyzed the expression of N-glycans in brain tissue from neurological mutant mice. In this paper we report the detection of alterations in N-glycans, mainly in relation to BA-1 and BA-2, in the cerebrum and cerebellum of *staggerer*, *shiverer*, and *jimpy* mutants, by using differential display of glycans. Though the present method did not directly identify the functional significance of N-glycans, it serves as a significant step towards the fur-

*To whom correspondence should be addressed. Tel: +81-6-6850-5380, Fax: +81-6-6850-5383, E-mail: suhase@chem.sci.osaka-u.ac.jp

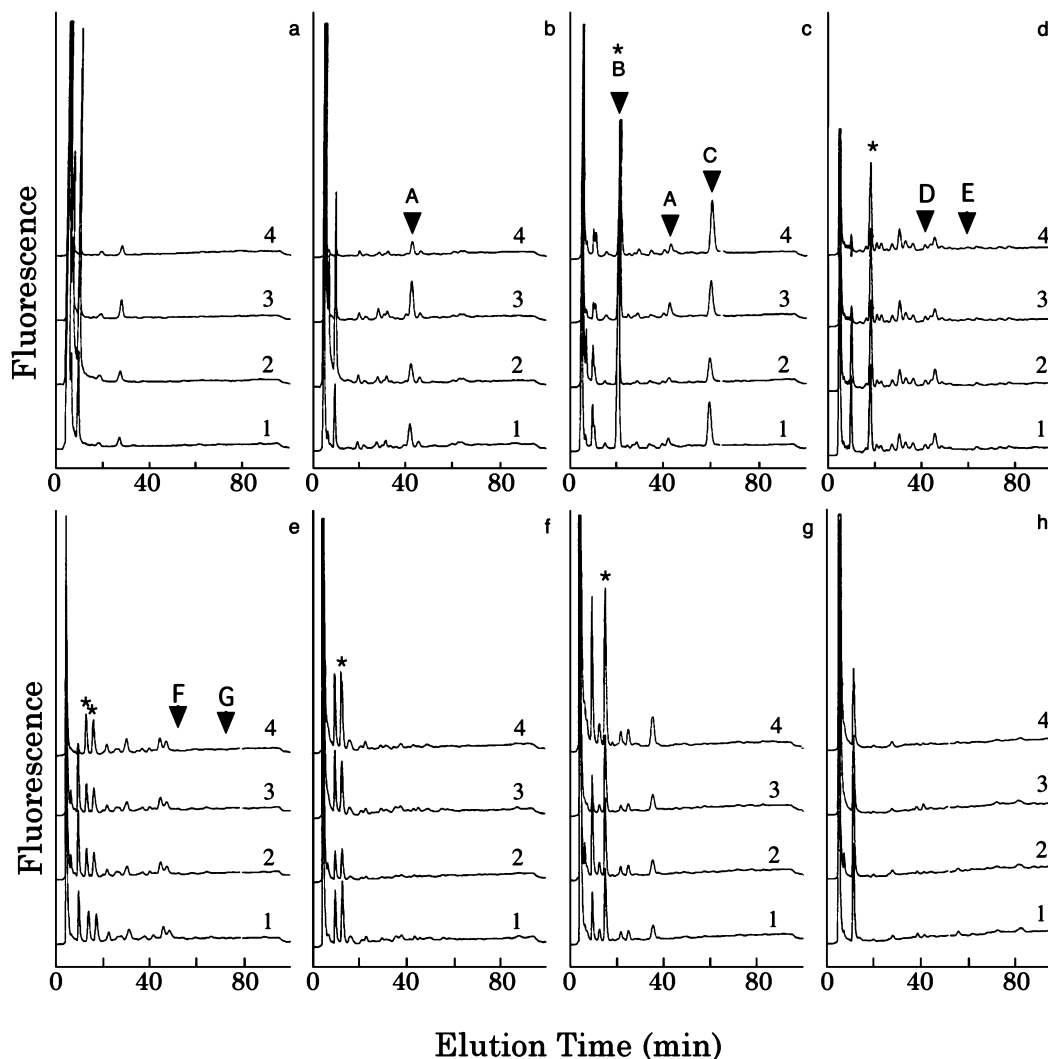


Fig. 1. HPLC elution profiles of Fractions N3–N10 from cerebrium. Fractions N3–N10 were obtained by size-fractionation HPLC and separated by reversed-phase HPLC. a, Fraction N3; b, Fraction N4, c, Fraction N5; d, Fraction N6, e, Fraction N7; f, Fraction N8, g, Fraction N9; h, Fraction N10. 1, HPLC profile of normal mice; 2,

HPLC profile of *jimpy* mice; 3, HPLC profile of *staggerer* mice; 4, HPLC profile of *shiverer* mice. Arrowhead A indicates the elution position of BA-1-PA; B, M5A-PA; C, BA-2-PA; D, BI-PA (42 min); E, BBS-PA (60 min); F, BIF-PA (55 min); G, BIBSF-PA (73 min). Asterisks indicate high-mannose type *N*-glycan.

ther understanding of the precise functions of *N*-glycans in the central nervous system. Of particular interest is the finding that some *N*-glycans were specifically expressed in mutant mouse brain.

MATERIALS AND METHODS

Materials—The mutant mice were of B6/C3 hybrid background. Normal mice were of the ICR strain. TSK-gel HW-40F and TSK-gel Amide-80 were purchased from Tosoh (Tokyo), YMC-Gel Sil S-5 was obtained from Yamamura Kagaku (Kyoto), Shodex Asahipak NH2P-50 was obtained from Showa Denko (Tokyo), and a Mono Q 5/5 HR column was obtained from Pharmacia (Uppsala, Sweden). Further materials included Cosmosil 5C18-P from Nacalai Tesque (Kyoto), anhydrous hydrazine from Tokyo Chemical Industry (Tokyo), 2-aminopyridine and dimethylamine-borane complex from Wako (Osaka), sialidase (*Arthrobacter ureafaciens*) from Nacalai Tesque,

and β -galactosidase (*Streptomyces* 6644k) from Seikagaku Kogyo (Tokyo). A mixture of PA-sialo *N*-glycans was prepared as reported previously from α_1 -acid glycoprotein obtained from Sigma (13).

Preparation of PA-*N*-Glycans—PA-*N*-Glycans were prepared from cerebrum and cerebellum of 3-week-old normal and mutant mice as described previously (8, 14). Cerebrums and cerebellums were extirpated from three male mice and thoroughly homogenized and lyophilized. A part of each lyophilized sample (2 mg) was hydrazinolyzed at 100°C for 10 h, then *N*-acetylated. The reducing ends of the liberated *N*-glycans were pyridylaminated using a Palstation model 1000 (Takara Biomedicals, Kyoto) under the conditions reported previously (9). Excess reagents were removed by gel filtration on a TSK-gel HW-40F column (1.5 × 20 cm) equilibrated with 10 mM ammonium acetate, pH 6.0 (15).

Exoglycosidase Treatment—PA-*N*-glycans prepared from 2 mg of lyophilized cerebrum or cerebellum were treated

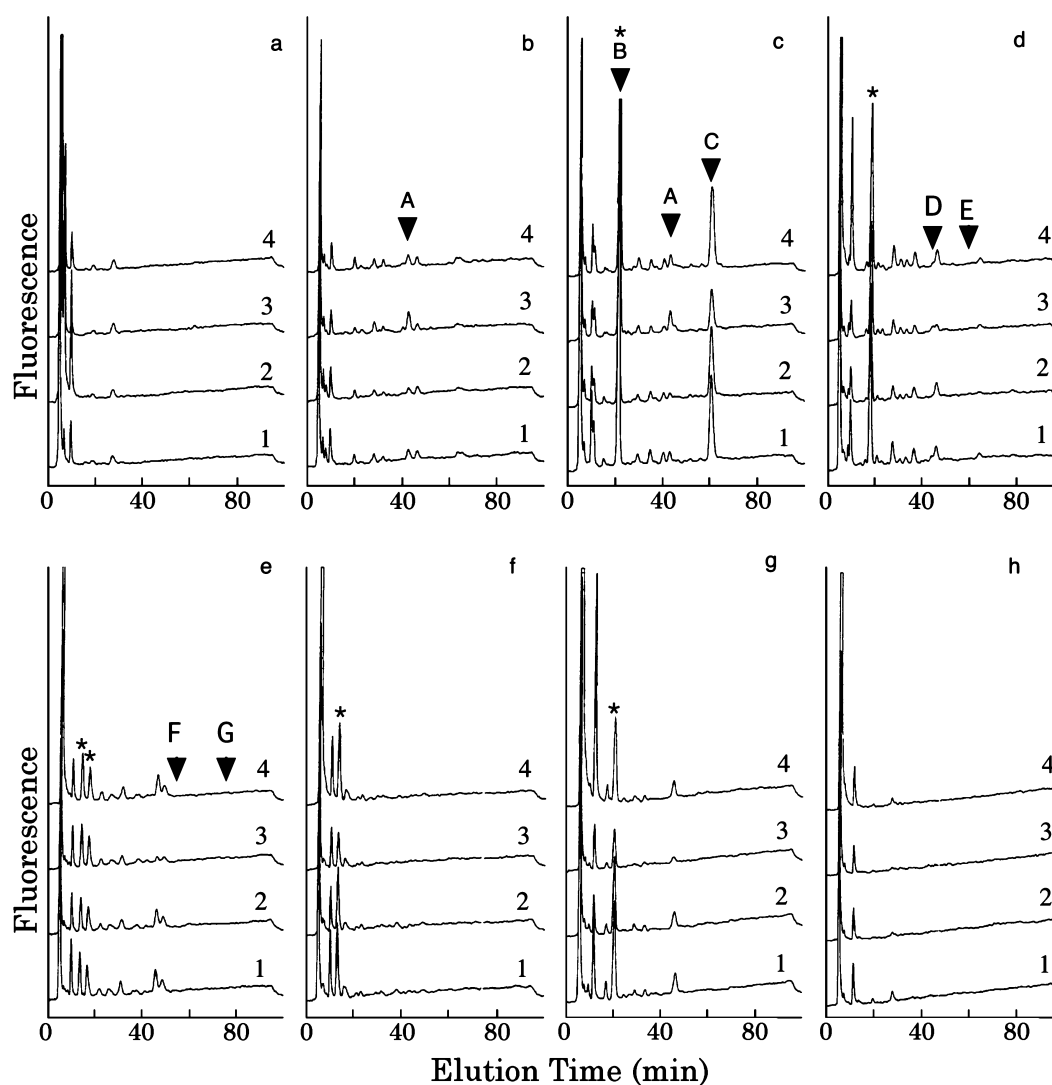


Fig. 2. HPLC elution profiles of Fractions N3–N10 from cerebellum. Fractions were obtained by size-fractionation and were sep-

arated by reversed-phase HPLC. Arrowheads, asterisks, letters and numerals are given in the legend to Fig. 1.

with 5 milliunits of *Arthrobacter* sialidase in 50 μ l of 50 mM ammonium acetate buffer, pH 5.0, at 37°C for 16 h. A PA-N-glycan (0.2 pmol) was incubated with 5 milliunits of galactosidase in 50 mM citrate-phosphate buffer, pH 3.5, in a total volume of 30 μ l at 37°C for 17 h. The enzymatic reaction was terminated by heating the digests at 100°C for 2 min.

High Performance Liquid Chromatography—A Shiseido Nanospace SI-1 liquid chromatograph was used during this study. Reversed-phase HPLC was performed on a Cosmosil 5C18-P column (0.15 \times 25 cm) with two eluents, A and B. Eluent A was 20 mM ammonium acetate buffer, pH 4.0, and Eluent B 20 mM ammonium acetate buffer, pH 4.0, containing 0.5% 1-butanol. The column was equilibrated with 15% Eluent B. After injection of a sample, the proportion of Eluent B was increased in a linear manner from 15 to 85% during a period of 90 min at a flow rate of 0.15 ml/min at 25°C. Size-fractionation HPLC was carried out on a TSK-gel Amide-80 column (0.46 \times 7.5 cm) with a guard column of YMC-Gel Sil-5 (0.75 \times 7.5 cm) to prevent damage to the Amide 80 column. Size-

fractionation HPLC was performed on an Amide 80 column at a flow rate of 1.0 ml/min. Two eluents, C and D, were used during the size fractionation. Eluent C was acetonitrile:water:acetic acid (85:15:3, v/v/v) titrated to pH 7.3 with triethylamine, and Eluent D was water:acetic acid (100:3, v/v) titrated to pH 7.3 with triethylamine. The column was equilibrated with Eluent C. After injecting a sample, the proportion of Eluent D was increased in a linear manner to 10% over a period of 2 min, and then to 40% over a period of 22 min (9). Size-fractionation HPLC using a Shodex Asahipak NH2P-50 column (0.2 \times 15 cm) was performed at a flow rate of 0.075 ml/min. Two eluents, E and F, were used. Eluent E was acetonitrile:water:acetic acid (950:50:3, v/v/v) titrated to pH 7.0 with 7 M aqueous ammonia; Eluent F was acetonitrile:water:acetic acid (200:800:3, v/v/v) titrated to pH 7.0 with 7 M aqueous ammonia. The column was equilibrated with 5% Eluent F. After injecting a sample, Eluent F was increased in a linear manner to 14% over a period of 3 min, to 25% over a period of 17 min, to 50% over a period of 60 min, and then finally to 75% over a 5-min period (12).

Abbreviation	Structure
BA-1	GlcNAc β 1-2Man α 1 GlcNAc β 1-4Man β 1-4GlcNAc β 1-4GlcNAc Fuc α 1-6GlcNAc
BA-2	Man α 1-6GlcNAc β 1-2Man α 1 GlcNAc β 1-4Man β 1-4GlcNAc β 1-4GlcNAc Fuc α 1-6GlcNAc GlcNAc β 1-2Man α 1
BIBSF	Gal β 1-4GlcNAc β 1-2Man α 1 GlcNAc β 1-4Man β 1-4GlcNAc β 1-4GlcNAc Fuc α 1-6GlcNAc
BIBS	Gal β 1-4GlcNAc β 1-2Man α 1 GlcNAc β 1-4Man β 1-4GlcNAc β 1-4GlcNAc
BIF	Gal β 1-4GlcNAc β 1-2Man α 1 GlcNAc β 1-4Man β 1-4GlcNAc β 1-4GlcNAc Fuc α 1-6GlcNAc
BI	Gal β 1-4GlcNAc β 1-2Man α 1 GlcNAc β 1-4Man β 1-4GlcNAc β 1-4GlcNAc
226-T	Gal β 1-4GlcNAc β 1-2Man α 1 GlcNAc β 1-4Man β 1-4GlcNAc β 1-4GlcNAc Man α 1-6GlcNAc β 1-2Man α 1
M9A	Man α 1-2Man α 1-6Man α 1 Man α 1-2Man α 1-3Man α 1 Man β 1-4GlcNAc β 1-4GlcNAc
M8A	Man α 1-2Man α 1-6Man α 1 Man α 1-3Man α 1-6Man α 1 Man β 1-4GlcNAc β 1-4GlcNAc
M7A	Man α 1-6Man α 1 Man α 1-2Man α 1-3Man α 1 Man β 1-4GlcNAc β 1-4GlcNAc
M7B	Man α 1-2Man α 1-6Man α 1 Man α 1-3Man α 1-6Man α 1 Man β 1-4GlcNAc β 1-4GlcNAc
M6B	Man α 1-6Man α 1 Man α 1-3Man α 1-6Man α 1 Man β 1-4GlcNAc β 1-4GlcNAc
M5A	Man α 1-6Man α 1 Man α 1-3Man α 1-6Man α 1 Man β 1-4GlcNAc β 1-4GlcNAc

Fig. 3. Structures and abbreviations of *N*-glycans used.

Separation of PA-*N*-glycans on an anion-exchange column was done on a Mono-Q column at the flow rate of 1.0 ml/min using two eluents, Eluent G and Eluent H. Eluent G was water titrated to pH 9.0 with 1 M aqueous ammonia and Eluent H 0.5 M titrated with ammonium acetate solution, pH 9.0. The column was equilibrated with Eluent G. After injecting a sample, Eluent H was increased in a linear manner to 10% during a period of 3 min, 40% during a period of 14 min, and 100% during a further 5 min period (16). PA-*N*-glycans were quantified with HPLC by using standard PA-GlcNAc.

Two-Dimensional Sugar Mapping—The structures of the PA-*N*-glycans were assessed by two-dimensional

sugar mapping. The elution positions of more than 100 standard PA-*N*-glycans have already been reported, and the introduction of a reversed-phase scale made it possible to predict the elution positions even if standard PA-*N*-glycans were not available (17). PA-*N*-glycans were separated by reversed-phase HPLC and size-fractionation HPLC, and the elution position of each *N*-glycan was compared with those of standard PA-*N*-glycans on the two-dimensional sugar map. Then, each PA-*N*-glycan was digested with exoglycosidases, and the structures of the products were analyzed on a two-dimensional sugar map as reported previously (18).

RESULTS AND DISCUSSION

Quantitative Analysis of BA-1 and BA-2 in Cerebellum and Cerebrum from Mutant Mice—*N*-Glycans liberated from lyophilized cerebrum and cerebellum obtained from mutant and normal mice were pyridylaminated. In the present study, ICR mice were used as normal mice, based on earlier findings that the expression patterns of PA-*N*-glycans obtained from ICR, BALB/C, and B6 mice were the same in several independent experiments (data not shown). The PA-*N*-glycans were then separated by Mono Q chromatography into a neutral fraction (N) and mono- to penta-sialylated *N*-glycan-containing fractions (A1–A5, respectively) according to the elution positions of standard sialylated PA-*N*-glycans. The neutral fraction (N), which contained BA-1-PA and BA-2-PA, was next separated by size-fractionation HPLC. Fractions N3–N10 were collected according to the elution positions of standard Man₃GlcNAc₂-PA–Man₉GlcNAc₂-PA and each fraction was further separated by reversed-phase HPLC (Figs. 1 and 2). Reproducibility of the experiments was confirmed by obtaining the same expression patterns using the same procedures. Peaks A and C were identified as BA-1-PA and BA-2-PA respectively, by comparing their elution positions with those of standard samples. Peak A was eluted in both Fraction N4 and N5 by size fractionation HPLC. The ratio of BA-1-PA to BA-2-PA obtained from the cerebrum of the *staggerer* mutant (1.5) was larger than that of *shiverer* mutant mice (0.4), *jimpy* mutant mice (0.9), and normal mice (0.7). BA-1 lacks the GlcNAc residue on the Man α 1-3 branch of BA-2 (Fig. 3), and the hydrolysis of this residue is considered to be caused by β -*N*-acetylhexosaminidase B, based on the finding that no BA-1 peak was obtained from knockout mice of β -*N*-acetylhexosaminidase (19). These results indicate that the activity of β -*N*-acetylhexosaminidase B in the cerebrum of *shiverer* mutant mice was lower, and that of *staggerer* mutant mice was higher, than that of normal mice. In cerebellum, the ratio of BA-1-PA to BA-2-PA in *staggerer* (0.9) was larger than that of *shiverer* mice (0.3), *jimpy* mice (0.2), and normal mice (0.2) (Fig. 2, b and c). These results suggest that β -*N*-acetylhexosaminidase B activity in the brain of *staggerer* mice was higher than in other mice tested, including normal mice. These results are compatible with the previous report indicating that the activity of β -*N*-acetylhexosaminidase in cerebellum of *staggerer* mouse was higher than that of a normal mouse (20). As the specific increase in the amount of BA-2 occurred during developmental phases associated with myelination and maturation of the dendritic tree in

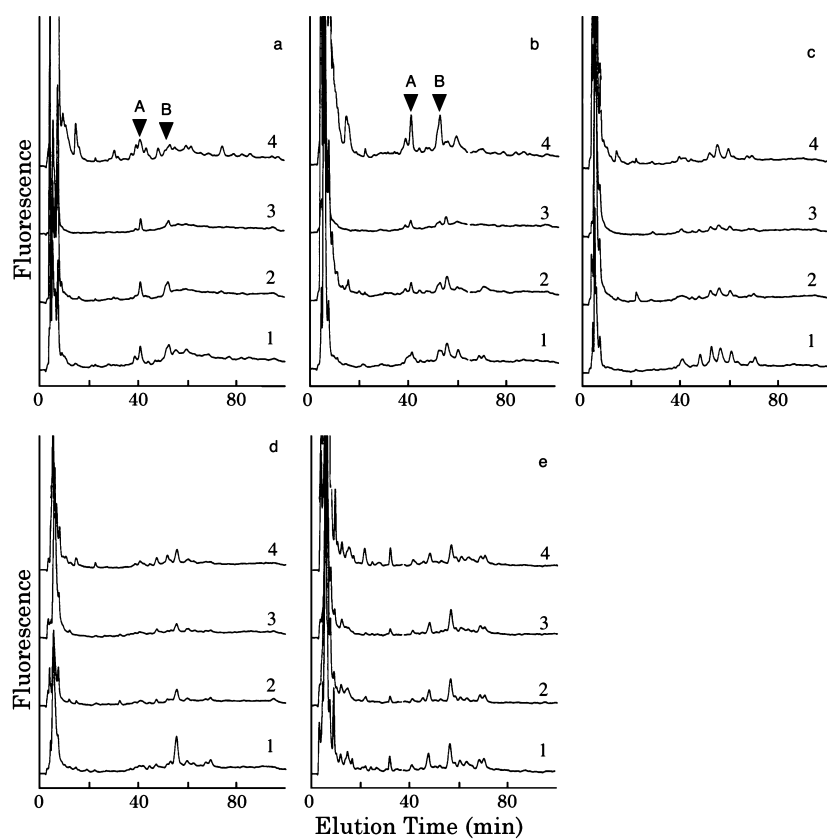


Fig. 4. HPLC elution profiles of Fractions A1N-A5N from cerebrum. Fractions were obtained by Mono Q HPLC, digested with sialidase, and the products were separated by reversed-phase HPLC. a, A1N; b, A2N; c, A3N; d, A4N; e, A5N. Arrowhead A indicates the elution position of BI-PA; B, BIF-PA. Numerals are given in the legend to Fig. 1.

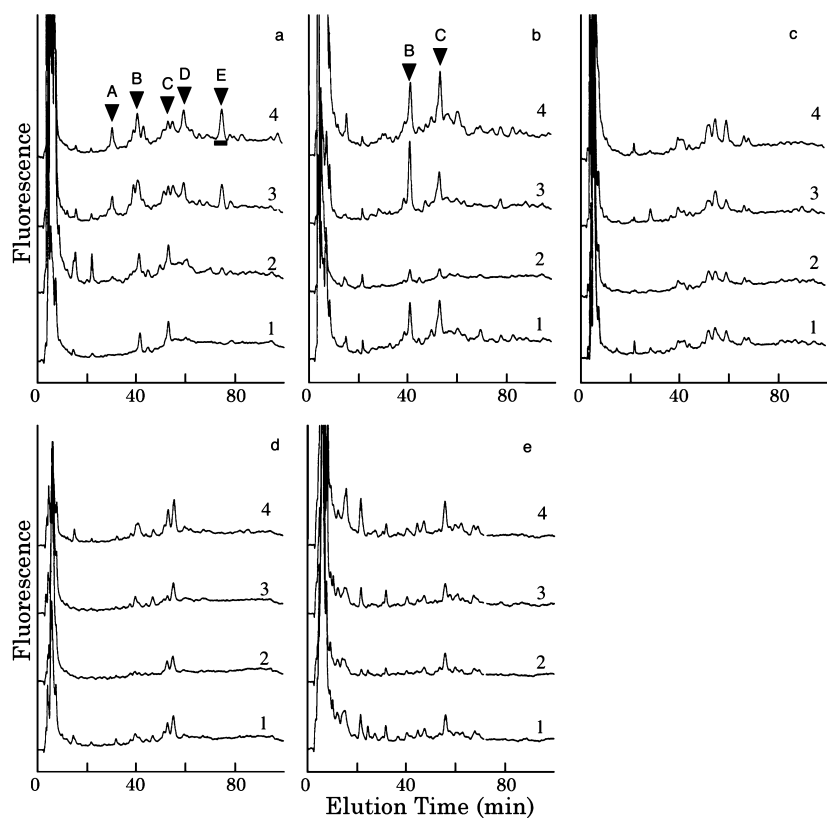


Fig. 5. HPLC elution profiles of Fractions A1N-A5N from cerebellum. Fractions were obtained by Mono Q HPLC and were separated by reversed-phase HPLC. Numerals and letters are shown in the legend to Fig. 4. Arrowhead A indicates the elution position of 226-T-PA; B, BI-PA; C, BIF-PA; D, BIBS-PA; E, BIBSF-PA without a Gal residue. Peak E was collected as indicated by the bar.

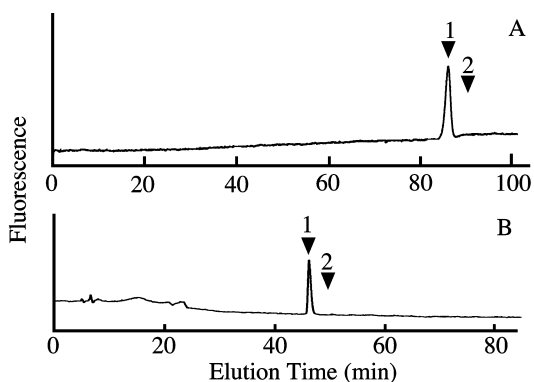


Fig. 6. HPLC elution profiles obtained after β 1-4galactosidase digestion of Fraction E in Fig. 5. A: Reversed-phase HPLC was performed on a Cosmosil 5C18P column (1.5 \times 250 mm). B: Size-fractionation HPLC was performed on a NH2P-50 column (2.0 \times 150 mm). The elution positions of PA-oligosaccharides are indicated by the arrows: 1, BA-2; 2, Fraction E and Gal-BA-2.

these mutant mice, and as BA-1 and BA-2 are specifically expressed in the cell membrane of mouse brain (8, 9), BA-1 and BA-2 may have some roles in the development of neural cells.

Detection of Other *N*-Glycans Specifically Expressed in Mutant Mouse Cerebrum and Cerebellum—Other *N*-glycans that are specifically expressed in mutant mice were next analyzed by comparing elution profiles of PA-*N*-glycans from normal and mutant mouse brain. The structure of each peak was assessed by comparing its elution position with those of standard PA-*N*-glycans. Most peaks appearing between 15 and 30 min in Fractions N5–N9 were high-mannose *N*-glycans (Figs. 1 and 2). Analysis by 2-dimensional mapping of high-mannose-type *N*-glycans indicated that they were M9A, M8A, M8B, M7A, M7B, M6B, and M5A; 2-dimensional maps suggested that the expression pattern of high-mannose-type *N*-glycan in the normal mouse were rather similar to those seen in mutant mice (data not shown). The substrate specificities of α -mannosidases that participate in the processing of high-mannose *N*-glycans in ER and Golgi have been reported previously (21–23). Based upon these data, the participation of α -mannosidases can be assessed by analyzing the isomeric structures of 12 oligomannose *N*-glycans (from Man₉GlcNAc₂–Man₅GlcNAc₂) that can be biosynthesized from glycoproteins, as all these high-mannose *N*-glycans can be separated by 2-dimensional sugar mapping (24). In these mice, sugar structures of glycoproteins were probably derived from M9A by digestion with ER-mannosidase I followed by Golgi α -mannosidase IA and IB, but with no contribution of Golgi α -mannosidase IC (25). These results suggested that the biosynthesis of high-mannose type *N*-glycans was not affected in mutant mice brain.

The asialo fractions (A1N–A5N), obtained by digesting the acidic fractions (A1–A5, respectively) with the sialidase, were analyzed by reversed-phase HPLC. The elution profiles of Fractions A3N, A4N, and A5N from normal and mutant mice cerebrum (Fig. 4) showed some small differences, but these peaks were not investigated further in the present study. Sialylated BI and BIF (Peak A and B, respectively) were larger in *shiverer* mice. Three

peaks, A, D, and E, remarkably appeared in *shiverer* and *staggerer* mouse cerebellum (Fig. 5). Peak A was identified as 226-T, Peak D as BIBS by 2-dimensional sugar mapping, and Peak E was eluted at the position of monogalactosylated BA-2-PA. As galactosylated BA-2 has not been detected in brain, Peak E from *shiverer* mice was further analyzed as follows. Peak E was digested with β -galactosidase, and the product was identified as BA-2 by 2-dimensional HPLC mapping, confirming that Peak E was Gal-BA-2 (Fig. 6). As galactosylated BA-2 was not detected in normal mice, this result implies that *shiverer* and *staggerer* mouse cerebellums exhibit disorders associated with the biosynthesis of *N*-glycans. *N*-Glycans having anionic residues like sialyl-galactosyl-BA-2 seemed to be expressed instead of the HNK-1 epitope, as HNK-1 antigen is lost in *staggerer* mouse cerebellum (26). *N*-Glycans with the HNK-1 epitope seemed to be eluted in Fraction A5, but these *N*-glycans were not studied further, as the alterations of *N*-glycans analyzed in the present paper related mainly to BA-1 and BA-2. The ratio of BIF to BI in *staggerer* mouse (0.4) was smaller than all other mice tested (0.8–1.2).

By comparing the HPLC profiles of PA-*N*-glycans obtained from mutant and normal mice, it became apparent that mutant-specific alterations of sugar structures were observed. These mutations were caused by the inactivation of genes which might affect the biosynthesis or the action of enzymes that synthesize and process *N*-glycans, resulting in the alterations of *N*-glycans detected in mutant mouse brain. However, it is unclear whether these differences derive from the alteration of proteins. As these observed alterations were specific to mutations, alteration of *N*-glycans might be related to the symptoms associated with these mutant mice.

This work was supported in part by the 21st Century COE (Creation of Integrated EcoChemistry), Protein 3000 programs, and the Japan Health Science Foundation.

REFERENCES

1. Matsumoto, M., Nakagawa, T., Inoue, T., Nagata, E., Tanaka, K., Tanaka, H., Minowa, O., Kuno, J., Sakakibara, S., Yamada, M., Yoneshima, H., Miyawaki, A., Fukuuchi, Y., Furuichi, T., Okano, H., Mikoshiba, K., and Noda, T. (1996) Ataxia and epileptic seizures in mice lacking type 1 inositol 1,4,5-trisphosphate receptor. *Nature* **379**, 168–171
2. Dautigny, A., Mattei, MG., Morello, D., Alliel, PM., Pham-Dinh, D., Amar, L., Arnaud, D., Simon, D., Mattei, JF., Guenet, JL., Jolles, P., and Avner, P. (1986) The structural gene coding for myelin-associated proteolipid protein is mutated in *jimpy* mice. *Nature* **321**, 867–869
3. Mikoshiba, K., Kohsaka, S., Takamatsu, K., and Tsukada, Y. (1981) Neurochemical and morphological studies on the myelin of peripheral nervous system from Shiverer mutant mouse: absence of basic proteins common to central nervous system. *Brain Res.* **204**, 445–460
4. Zanjani, H.S., Herrup, K., Guastavino, M., Delhaye, N., and Mariani, J. (1994) Developmental studies of the inferior olivary nucleus in staggerer mutant mice. *Brain Res. Dev. Brain Res.* **82**, 18–28
5. Bradley, P. and Berry, M., (1978) The Purkinje cell dendritic tree in mutant mouse cerebellum. A quantitative Golgi study of Weaver and Staggerer mice. *Brain Res.* **142**, 135–141
6. Rosenbluth, J. (1980) Central myelin in the mutant shiverer. *J. Comp. Neurol.* **194**, 639–648

7. Sidman, R.L., Dickie, M.M., and Appel, S.H. (1964) Mutant mice (quaking and jimpy) with deficient myelination in the central nervous system. *Science* **144**, 309
8. Shimizu, H., Ochiai, K., Ikenaka, K., Mikoshiba, K., and Hase, S. (1993) Structures of N-linked sugar chains expressed mainly in mouse brain. *J. Biochem.* **114**, 334–338
9. Nakakita, S., Natsuka, S., Ikenaka, K., and Hase, S. (1998) Development-dependent expression of complex-type sugar chains specific to mouse brain. *J. Biochem.* **123**, 1164–1168
10. Hoffmann, A., Nimitz, M., Wurster, U., and Conradt, H.S. (1994) Carbohydrate structures of β -trace ptotein from human cerebrospinal fluid: evidence for “brain-type” N-glycosylation. *J. Neurochem.* **63**, 2185–2196
11. Hoffmann, A., Nimitz, M., Getzlaff, R., Wurster, U., and Conradt, H.S. (1995) “Brain-type” N-glycosylation of asialo-transferrin from human cerebrospinal fluid. *FEBS Lett.* **359**, 164–168
12. Nakakita, S., Menon, K.K., Natsuka, S., Ikenaka, K., and Hase, S. (1999) β 1-4Galactosyltransferase activity of mouse brain as revealed by analysis of brain-specific complex-type N-linked sugar chains. *J. Biochem.* **126**, 1161–1169
13. Ushida, Y., Natsuka, S., Shimokawa, Y., Takatsu, Z., Shimamura, S., and Hase, S. (1997) Structures of the sugar chains of recombinant macrophage colony-stimulating factor in Chinese hamster overy cell. *J. Biochem.* **122**, 148–156
14. Hase, S., Ikenaka, T., and Matsushima, Y. (1978) Structure analysis of oligosaccharides by tagging of the reducing end sugars with a fluorescent compound. *Biochem. Biophys. Res. Commun.* **85**, 257–263
15. Kuraya, N. and Hase, S. (1992) Release of O-linked sugar chains from glycoproteins with anhydrous hydrazine and pyridylation of the sugar chains with improved reaction conditions. *J. Biochem.* **112**, 122–126
16. Yamamoto, S., Hase, S., Fukuda, S., Sano, O., and Ikenaka, T. (1989) Structures of the sugar chains of interferon- γ produced by human myelomonocyte cell line HBK-38. *J. Biochem.* **105**, 547–555
17. Yanagida, K., Ogawa, H., Omichi, K., and Hase, S. (1998) Introduction of a new scale into reversed-phase high-performance liquid chromatography of pyridylamino sugar chains for structural assignment. *J. Chromatogr. A* **800**, 187–198
18. Makino, Y., Omichi, K., and Hase, S. (1998) Analysis of sugar chain structures from the reducing end terminal by combining partial acid hydrolysis and a two-dimensional sugar map. *Anal. Biochem.* **263**, 172–179
19. Okamoto, Y., Omichi, K., Yamanaka, Y., Ikenaka, K., and Hase, S. (1999) Conversion of brain-specific complex type sugar chains by N-acetyl- β -D-hexosaminidase B. *J. Biochem.* **125**, 537–540
20. Wille, W., Heinlein, U.A.O., Spier-Michl, I., Thielsch, H. and Trenkner, E. (1983) Development-dependent regulation of N-acetyl- β -D-hexosaminidase of cerebellum and cerebrum of normal and staggerer mutant mice. *J. Neurochem.* **40**, 235–239
21. Bischoff, J., Liscum, L., and Kornfeld, R. (1986) The use of 1-deoxymannojirimycin to evaluate the role of various α -mannosidases in oligosaccharide processing in intact cells. *J. Biol. Chem.* **261**, 4766–4774
22. Tabas, I. and Kornfeld, S. (1979) Purification and characterization of a rat liver Golgi α -mannosidase capable of processing asparagine-linked oligosaccharides. *J. Biol. Chem.* **254**, 11655–11663
23. Kornfeld, R. and Kornfeld, S. (1985) Assembly of asparagine-linked oligosaccharides. *Annu. Rev. Biochem.* **54**, 631–664
24. Hase, S., Natsuka, S., Oku, H., and Ikenaka, T. (1987) Identification method for twelve oligomannose-type sugar chains thought to be processing intermediates of glycoproteins. *Anal. Biochem.* **167**, 321–326
25. Tremblay, L.O. and Herscovics, A. (2000) Characterization of a cDNA encoding a novel human golgi α 1, 2-mannosidase (IC) involved in N-glycan biosynthesis. *J. Biol. Chem.* **275**, 31655–31660
26. Chou, D.K., Flores, S., and Jungalwala, F.B. (1990) Loss of sulfoglucuronyl and other neolactoglycolipids in Purkinje cell abnormality murine mutants. *J. Neurochem.* **54**, 1589–1597